Journal of Asian Earth Sciences 65 (2013) 13–20

Contents lists available at SciVerse ScienceDirect

Journal of Asian Earth Sciences

journal homepage: www.elsevier.com/locate/jseaes

Origins of natural gases from marine strata in Northeastern Sichuan Basin (China) from carbon molecular moieties and isotopic data

Yunpeng Wang [a,*], Changyi Zhao [b], Hongjun Wang [b], Zhaoyun Wang [b], Zecheng Wang [b]

[a] State Key Laboratory of Organic Geochemistry, Guangzhou Institute of Geochemistry, Chinese Academy of Sciences, Guangzhou, Wushan 510640, China
[b] Research Institute of Petroleum Exploration and Development, PetroChina, Beijing 100083, China

ARTICLE INFO

Article history:
Available online 27 September 2012

Keywords:
Gas origin
Carbon molecular moieties
Carbon isotope
Geochemical diagram
Eastern Sichuan
Oil cracking
Residual kerogen
Thermal Sulfate Reduction

ABSTRACT

To determine the origin, maturity, formation mechanism and secondary process of marine natural gases in Northeastern Sichuan area, molecular moieties and carbon isotopic data of the Carboniferous and Triassic gases have been analyzed. Typical samples of marine gas precursors including low-maturity kerogen, dispersed liquid hydrocarbons (DLHs) in source rocks, residual kerogen and oil have been examined in a closed system, and several published geochemical diagrams of gas origins have been calibrated by using laboratory data. Results show that both Carboniferous and Triassic gases in the study area have a thermogenic origin. Migration leads to stronger compositional and weak isotopic fractionation, and is path dependent. Carboniferous gases and low-H_2S gases are mainly formed by secondary cracking of oil, whereas high-H_2S gases are clearly related to the TSR (Thermal Sulfate Reduction) process. Gases in NE Sichuan show a mixture of heavy (^{13}C-enriched) methane in comparison to the lower maturated ethane of Triassic gas samples, suggesting a similar source and maturity for ethane and propane of Carboniferous gases, and a mixture of heavy ethane to the propane for Triassic gases. Based on the data plotted in the diagram of Chung et al. (1988), the residual kerogen from Silurian marine shale and palaeo oil reservoirs are the main source for Carboniferous gases, and that the residual kerogen from Silurian and Permian marine rocks and Permian paleao oil reservoirs constitute the principal source of Triassic gases.

1. Introduction

The Sichuan Basin is the largest basin in China with the largest natural gas reserves and production, especially in the marine strata in the northeastern areas (Xie et al., 2000). Marine gas reserves account for 70% of the production in the whole basin (Zhang and Zhu, 2006). Gases have been discovered in marine strata from Silurian to Jurassic, but most gas reservoirs are found in the Carboniferous *Huanglong* formation, Permian *Changxing* formation, and Lower Triassic *Feixianguan* formation. Currently, seven large gas fields with gas reserves larger than 30 billion cubic meters have been discovered in marine strata of Northeastern Sichuan (Table 1), the *Wolonghe*, *Wubaiti*, *Shapingchang*, *Luojiazhai*, *Dukouhe*, *Tieshanpo* and *Puguang* gas fields (Dai et al., 2008). Wang et al. (2004) recognized that the natural gases of marine strata in eastern Sichuan originated from secondary cracking of previously formed oil, though some studies argue different viewpoints (Zhao et al., 2006; Ma et al., 2008). Besides oil cracking, highly maturated residual kerogen is regarded as another very important source for natural gases in the Carboniferous strata in Eastern areas whereas TSR (Thermal Sulfate Reduction) is considered to be very important for the formation of highly maturated methane in Triassic strata in the Northeastern areas (Zhao et al., 2006; Ma et al., 2008). Analysis of the carbon molecular moieties and isotopic composition of gas samples indicates that most Carboniferous and Triassic natural gasses show extensive mixing (Wang et al., 2008). Because of the high maturity of both gases and source rocks, the origin and formation mechanism of marine natural gases in NE Sichuan area are complicated and less studied. Compared to secondary cracking of oil, the contribution of primary cracking of highly-maturated residual kerogen and roles of TSR and other post-reservoir alternation process such as migration and mixing are still not well understood. In addition, there exist multiple layers of source rocks overlaying each other, making the petroleum reservoir systems complex, and the post-Triassic transition from marine to terrestrial deposition adjusted source-reservoir layout (Ma et al., 2008). It is therefore of significance to study the origin of marine natural gases and characterize the impact of secondary processes. In this study, carbon molecular moieties and isotopic data of Carboniferous and Triassic gases as well as some molecular and isotopic diagrams were constructed to identify gas origin, to estimate gas maturity, and probe the impact of late stage of tectonic evolution.

* Corresponding author. Address: P.O. Box 1131, Guangzhou, Wushan 510640, China. Tel./fax: +86 20 85290197.
E-mail address: wangyp@gig.ac.cn (Y. Wang).

1367-9120/$ - see front matter © 2012 Elsevier Ltd. All rights reserved.
http://dx.doi.org/10.1016/j.jseaes.2012.09.015

Table 1
List of seven large (>30 billion m^3) gas fields (Dai et al., 2008; Ma et al., 2008).

Gas field	Strata symbol the reservoir rock	Gas reserves (Billion M^3)
Wolonghe	C, P_1, P_2, T_1	44.6
Wubaiti	C, P	58.7
Shapingchang	C, P_1, P_2, T_1	39.7
Luojiazhai	$T_{1f,}$ T_{1j}	72.1
Dukouhe		35.9
Tieshanpo		37.4
Puguang	T_{1f}	356

2. Geological setting and method

The Sichuan Basin is situated in the southwestern part of China (Fig. 1). The marine deposits in Northeastern Sichuan dating from Sinian of later Proterozoic to earlier Carboniferous are mainly carbonate (Fig. 2), among which the lower Silurian strata (S_1) consisting mainly of dark shale deposited on a wide shelf with TOC = 0.6–1.6% (Hu, 1997). The whole area uplifted during the Caledonian orogeny, and the Devonian and early Carboniferous strata have been abraded. During late stage Caledonian movement, the whole NE Sichuan experienced a transgression as manifested by a sequence of mudflat carbonates (C_{2h}, *Huanglong* Formation) with 40–50 m residual depth. At the end of the Carboniferous, the area was uplifted again and the top part of C_{2h}, i.e., the Upper Carboniferous, was strongly weathered forming abundant secondary pores becoming important reservoir rocks in eastern Sichuan. From Permian to Triassic, the area experienced a new deposition cycle including Permian reef carbonates, slope clastics, and thin coal seams followed by earlier Triassic oolitic carbonates in the northeastern area, forming another important reservoir rock in NE Sichuan.

As far as tectonic controls and trap properties are concerned, Carboniferous and Triassic gas pools exhibit different characteristics: Carboniferous traps are mainly anticlines whereas Triassic traps are mainly fault-controlled (Hu, 1997). The later Himalayan movement significantly influenced both Carboniferous and Triassic gas pools, reworking the Carboniferous traps into steep anticlines, and the Triassic ones into fault-sealed ones (Wang et al., 2004). In this study, we sampled Carboniferous gas from *Wubaiti*, *Shapinchang* and *Wolonghe* in eastern Sichuan area and Triassic gas from *Liujiazhai*, *Tieshanpo* and *Dukouhe* in Northeastern Sichuan area. The molecular moieties, C_1, C_2, and C_3, and carbon isotopes were analyzed in laboratory by gas chromatograph (GC) and gas chromatograph isotope ratio mass-spectrometer (GC-IRMS). The chemical and isotopic compositions of gas samples are listed in Table 2. For comparison, some published data of gas chemical and isotopic compositions were also used for plotting.

We calibrated several published geochemical diagrams of gas origins using our laboratory data in this study. Laboratory pyrolysis was carried out in a closed system on gas generated from typical samples of marine gas precursors including low-maturity kerogen, dispersed liquid hydrocarbon (DLH) in source rocks, residual kerogen, and oil. These samples included low-maturity kerogen, dispersed liquid hydrocarbon (DLH) in source rocks, residual kerogen and in-reservoir oil. Geochemical characteristics of both source rocks and oil for laboratory simulation are listed in Table 3. From these basic chemical and isotopic as well as their maturities, they can be easily classified as type II (marine origin) kerogen. The molecular moieties and isotopic compositions of pyrolysis gases from these samples were analyzed and used for diagram calibration to identify the origin of the gas, estimate gas maturity and probe the impact of secondary processes. Our pyrolysis apparatus consists of a closed, temperature-programmed (non-isothermal), gold-tube system described by Wang et al. (2006). The experiments were carried out at heating rates of 2 °C/h and 20 °C/h. Pyrolysis procedures and analysis have been described in detail by Wang et al. (2006, 2007). In a closed system, the liquid hydrocarbon and residual kerogen of marine source rocks mix together in hydrocarbon generation, making it difficult to discriminate the two types of gases. We therefore performed separate experiments for the generation of liquid hydrocarbon and residual kerogen. We first carried out kinetic experiments for low-maturity kerogen by heating to the temperature range between liquid hydrocarbon generation and cracking (390–400 °C for this sample). Next we

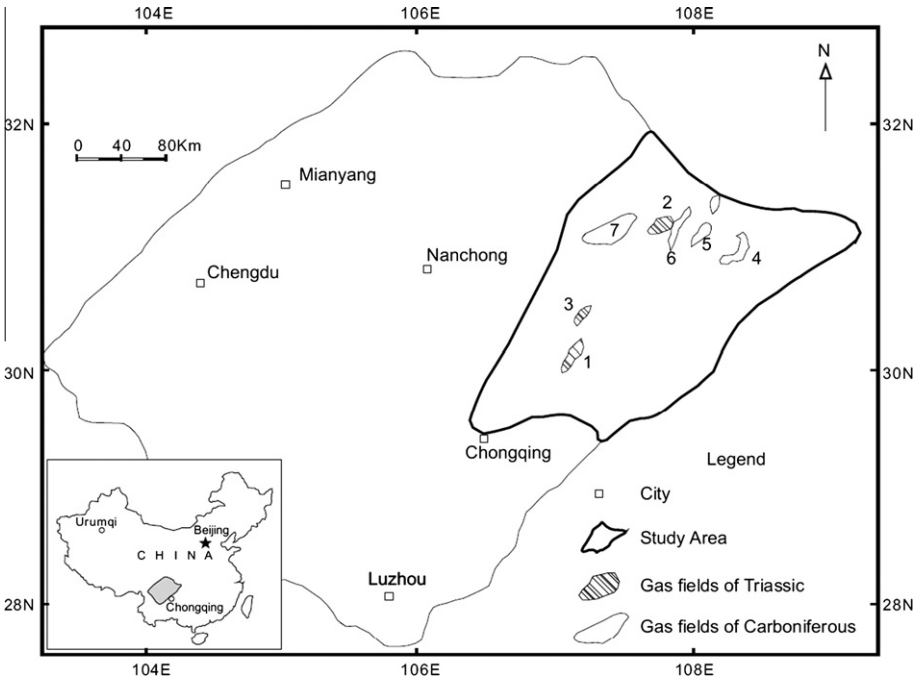

Fig. 1. Map of the Sichuan Basin showing its location in China, the study area and gas fields (1. Wolonghe; 2. Wobaiti; 3. Shapingchang; 4. Luojiazhai; 5. Dukouhe; 6. Tieshanpo; 7. Puguang. Here, C refers Carboniferous; T refers Triassic).

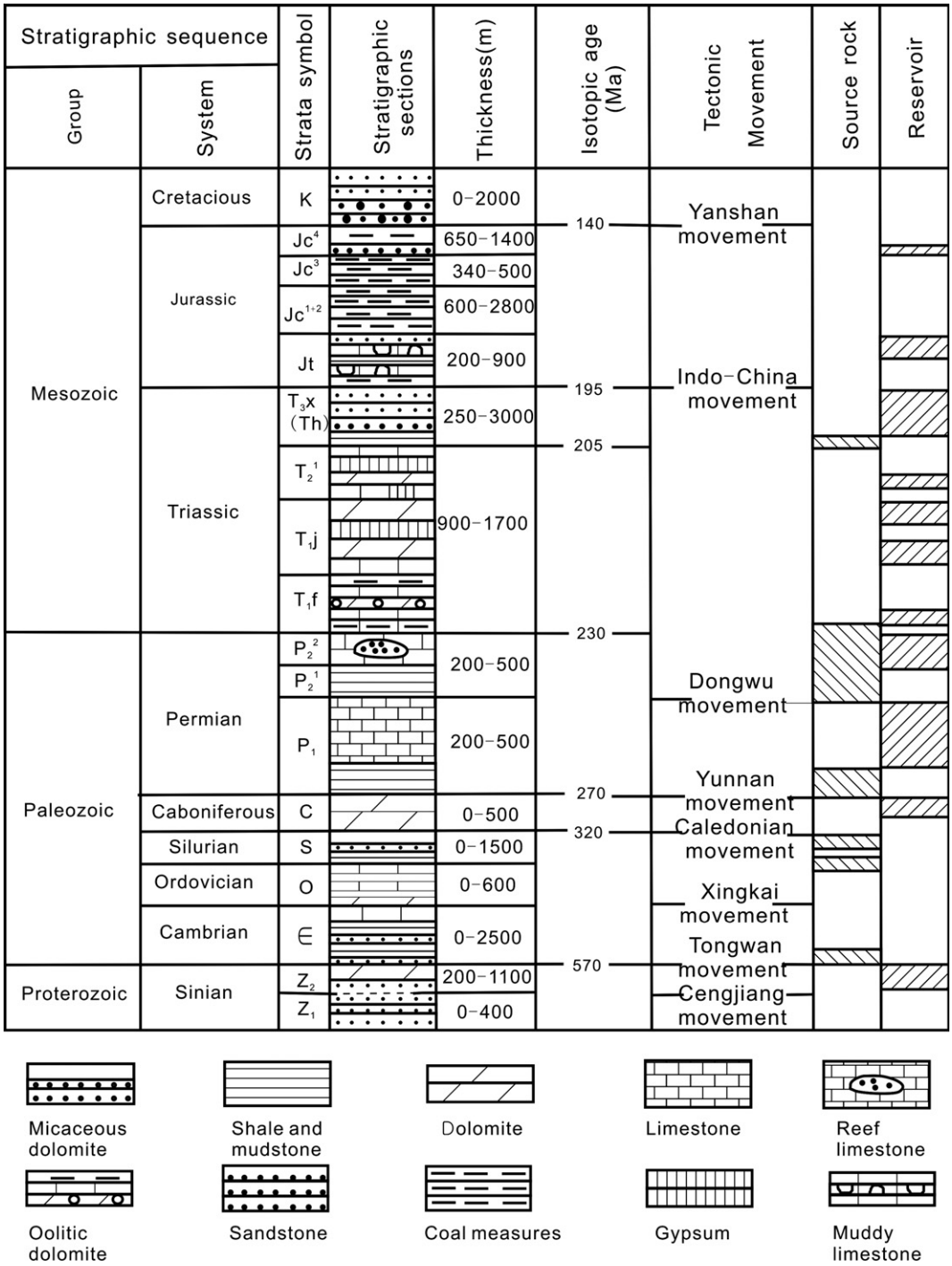

Fig. 2. Stratigraphic sequences of Sichuan Basin (the Devonian and early Carboniferous strata have been abraded in NW Sichuan area, Wang et al., 2001).

physically separated the residual kerogen and liquid hydrocarbon (bitumen) by chloroform extraction. Both the extracts and residual kerogen were used for kinetic experiments of gas generation under the same experimental conditions.

3. Results and discussions

3.1. Gas origin and migration

Diagram of $C_1/(C_2 + C_3)$ ratios and carbon isotope compositions of methane ($\delta^{13}C_1$) are widely used to distinguish between biogenic and abiogenic gases (Bernard et al., 1978). Generally, abiogenic (inorganic) gases have $\delta^{13}C_1$ value heavier than −20‰ in Fig. 3. As illustrated in Fig. 3, the $\delta^{13}C_1$ value of both Carboniferous and Triassic gases range between −30‰ to −40‰ suggesting that all gases have a biogenic origin including microbial or thermogenic ones. Based on $\delta^{13}C_1$ value in Fig. 3, most gases can be genetically classified as thermogenic gases because of the relatively high $C_1/(C_2 + C_3)$ ratios. This suggests that gas dryness ($C_1/(C_2 + C_3)$) is mainly controlled by simultaneous maturation and migration. However, the isotopic fraction is not as pronounced as the $C_1/(C_2 + C_3)$ ratio, indicating that gas migration will not enhance isotopic fractionation. Compositional fractionation of Triassic gases is more apparent than that of Carboniferous gases. One reason is

Table 2
Chemical and isotopic compositions of gas samples from Carboniferous (C_2) and Triassic (T_{3f}), NE Sichuan.

Well	Strata	C_1 (%)	C_2 (%)	C_3 (%)	$\delta^{13}C_1$ (‰)	$\delta^{13}C_2$ (‰)	$\delta^{13}C_3$ (‰)
TD-1	C_2	97.38	0.5	0.06	−32.36	−37.27	−34.21
WQ1	C_2	95.49	1.26	0.55	−36.46	−30.32	−25.28
Wo2	C_2	92.74	0.84	0.22	−32.77	−28.71	−23.53
Wo25	C_2	92.46	0.82	0.21	−33	−28.98	−24.18
Wo3	C_2	94.41	0.76	0.17	−32.68	−28.92	−24.29
Wo94	C_2	97.05	0.88	0.11	−32.4	−36.9	−33.2
Wo48[a]	C_2	97.16	0.46	0.05	−32.4	−35.7	
Wo52[a]	C_2	99	0.2	0.018	−32.1	−35.3	−30.5
Wo58[a]	C_2	97.13	0.46	0.05	−32.3	−36.3	−27.1
Wo65[a]	C_2	98.9	0.32	0.015	−32.1	−36.1	−32
Wo85[a]	C_2	98.4	0.35	0.026	−32.1	−36.3	
Wo96	C_2	97.51	0.05	0.05	−33	−35.5	
Wo120	C_2	96.4	0.65	0.06	−32.1	−36.1	−32
Wo88	C_2	97.02	0.52	0.06	−32.7	−34.6	−31.5
Wo127	C_2	93.86	0.53	0.02	−33.2	−35.8	−33.4
Guan2	C_2	97.39	0.36	0.03	−31.14	−34.94	
Guang7	C_2	97.65	0.38	0.02			
TD55	C_2	97.07	0.87	0.26	−31.75	−36.17	
Guan10	C_2	96.23	0.36	0.02	−31.67	−35.27	
LD3	C_2	96.81	0.34	0.02			
TD71	C_2	96.94	0.42	0.05			
Cheng18	C_2	95.97	0.45	0.02	−33.12	−36.27	
TS11	T_{3f}	97.99	0.23	0.01	−33	−35.2	
TS13	T_{3f}	98.23	0.25	0.01	−33	−34.7	
Cheng16	T_{3f}	98.38	0.35	0.02			
Xin12	T_{3f}	98.55	0.35	0.05			
TS5	T_{3f}	98.6	0.23	0.01	−32.09	−33.7	
Guan6	T_{3f}	98.65	0.35	0.02			
Cheng16	T_{3f}	98.75	0.37	0.02	−33.5	−37.4	
Du4	T_{3f}	98.78	0.19	0.01	−29.83	−32.39	
Cheng22	T_{3f}	98.84	0.25	0.01	−33.8	−36.5	
QL1	T_{3f}	98.85	0.38	0.02			
Cheng22	T_{3f}	98.92	0.25	0.01			
Guan23	T_{3f}	98.97	0.32	0.02			
LJ7	T_{3f}	81.37	0.07		−31.5	−29.4	
JZ1	T_{3f}	96.75	0.26	0.01			
Cao10	T_{3f}	96.85	0.53	0.38			
Xin9	T_{3f}	97.46	0.37	0.05			
TS21	T_{3f}	97.64	0.22	0.01			
Guan22	T_{3f}	97.75	0.28	0.01			
Cao8	T_{3f}	97.81	0.91	0.19			
TS11	T_{3f}	97.99	0.23	0.1			
BD5	T_{3f}	97.99	0.46	0.1			

[a] Cai et al. (2003).

Table 3
Geochemical characteristics of the typical samples for laboratory pyrolysis.

Area	Depth (m)	Type	Age	TOC (%)	S_2 (mg g^{-1})	T_{max} (°C)	HI (mg g^{-1})	R_0 (%)	Kerogen type
Zhangjiakou North China	Surface	Marine shale	Pt	3.96	20.11	430	507	0.56	IIa
		Kerogen	Pt	51.75	217.20	437	419	0.56	IIa
Well LG-1, Tarim Basin	4010	Marine oil	O	[a]SAT (%)	ARO (%)	ASPH (%)	RESIN (%)	δ^{13}Coil (‰)	Type II
				61.2	22.8	10.8	5.2	−33.2	II

[a] The value represents the group fractions of oil composition in percentage (SAT: saturated hydrocarbon, ARO: aromatic hydrocarbon, ASPH: asphaltene, RESIN: resin).

that they have different structures of gas traps and migration paths. The migration paths for gasses from Carboniferous pools are mainly through pores of weathered carbonate whereas those for Triassic pools are fault cracks (Dai et al., 2008; Ma et al., 2008), which may be another reason controlling the migration fraction. TSR will also promote the gas dryness increasing, which may be another important control for Triassic gases. We will discuss it later.

3.2. Gas formation mechanism

We used as model for the gas formation mechanisms the genetic fractionation for thermogenic gases expressed as the $\ln(C_1/C_2)$ versus $\ln(C_2/C_3)$ diagram as proposed by Prinzhofer and Huc (1995). Such plot allows differentiation between gases generated by primary cracking of kerogen (sub-vertical trend) and gases generated by secondary cracking of oils (sub-horizontal trend). According to Prinzhofer and Huc (1995), ratios of C_1/C_2 and C_2/C_3 exhibit different variation trends regardless of diffusion, migration, and retention because $\ln(C_1/C_2)$ and $\ln(C_2/C_3)$ only depend on the properties and maturities of source rocks. The range of $\ln(C_1/C_2)$ for the primary cracking gases from kerogen is larger relative to that of $\ln(C_2/C_3)$, whereas the range of $\ln(C_1/C_2)$ for secondary cracking gases from oil or DLH is smaller relative to that of $\ln(C_2/C_3)$.

Our previous study found that cracking gases from kerogen at both early and high maturity stages and gases form residual

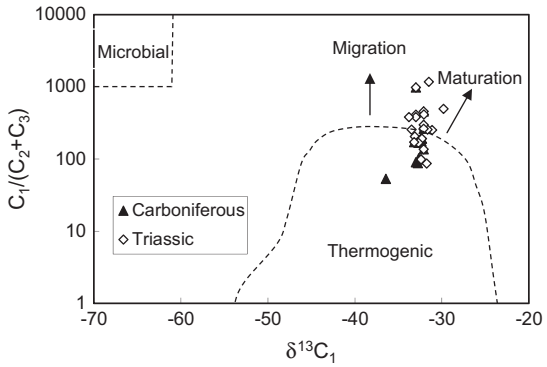

Fig. 3. Geochemical diagram of $\delta^{13}C_1$–$C_1/(C_2+C_3)$ of marine natural gases of the Northeastern Sichuan Basin after Bernard et al. (1978) to identify biogenic and abiogenic gases, as well as to show maturation, mixing and migration trends.

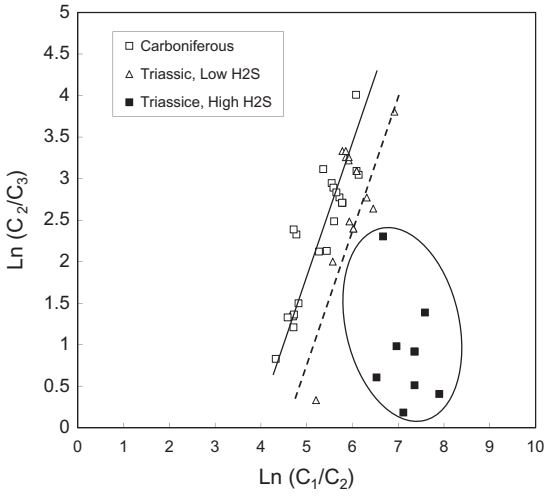

Fig. 4. Molecular ratios of gases of our case using $\ln(C_1/C_2)$ versus $\ln(C_2/C_3)$ diagram proposed by Prinzhofer and Huc (1995), differentiation of gases generated by primary cracking of kerogen (sub-horizontal trend) from gases generated by secondary cracking of oils (sub-vertical trend). Here, two lines are vertical showing secondary cracking of Carboniferous and high-H_2S Triassic gases while low-H_2S Triassic gases (in circular area) promote the conversion of heavy gases to methane.

kerogen exhibit the characteristics of primary cracking gases. The gas data plot along the increasing trend of $\ln(C_1/C_2)$ whereas oil and DLH-cracking gases exhibit the characteristics of secondary cracking gases and as the data plot along the increasing trend of $\ln(C_2/C_3)$. In general, marine kerogen exhibits the characteristics of primary cracking gases at the early and later maturity stages and those of secondary cracking gases in the medium maturity range (Wang et al., 2008). The diagram for our case study is shown in Fig. 4 (Wang et al., 2006, 2008, 2010). We found that all samples of Carboniferous and Triassic low-H_2S gases plotted along the secondary gases of oil. This indicates that they were mainly formed by secondary cracking of the oil. The Triassic high-H_2S gases plotted away from the vertical towards the direction of $\ln(C_1/C_2)$ increasing with $\ln(C_2/C_3)$ staying steady, which indicates an increase in methane and decrease in ethane. The increase of H_2S, clearly reflects Thermal Sulfate Reduction which promotes the cracking of heavy hydrocarbons including ethane into methane. It should be noted that the values of C_1/C_2 of natural gases from these two areas are far larger than those of simulated gases in the laboratory, suggesting as possible causes migration or mixing of gases with different origins and maturities.

3.3. Maturity and mixing

We used the isotopic composition of the individual gas components to determine gas maturity. They are a function of thermal maturity, isotopic composition of the source rock kerogen, and gas alteration history. In this study, an isotope-maturity model developed by Berner and Faber (1996) was used to estimate the type and maturity of the precursor (source) material. The modeled carbon isotopic ratios of methane, ethane, and propane are expressed in relation to source rock maturities as characterized by vitrinite reflectance. In this model, a selection mode allows the user to calibrate the maturity lines for a terrestrial and and/or for a marine (sapropelic) source rock, respectively, choosing the carbon isotope ratio for each precursor material.

According to the model, carbon isotope ratios of corresponding methane against ethane or ethane against propane (Fig. 5) should plot on or near the maturity line if both gases derived from one terrestrial or marine source rock (Berner and Faber, 1996). In our case, all samples for $\delta^{13}(C_1–C_2)$ diagram clearly plot above the projected maturity line indicating an admixture of heavy (^{13}C-enriched) methane to the lower maturated ethane, especially for the Triassic gas samples. The scattering of the δ^{13}C ethane values might represent source variations. Comparatively, all samples from Carboniferous strata for $\delta^{13}(C_2–C_3)$ diagram clearly plot alone the projected maturity line indicating that ethane and propane have the same source and maturities whereas samples from Triassic strata for $\delta^{13}(C_2–C_3)$ diagram plot somewhat above the projected maturity line indicating a slight admixture of heavy ethane to the propane. The scatter in δ^{13}C propane values may also reflect source variations. From these plots, the maturities of methane, ethane and propane can be estimated. The maturities of ethane and propane from

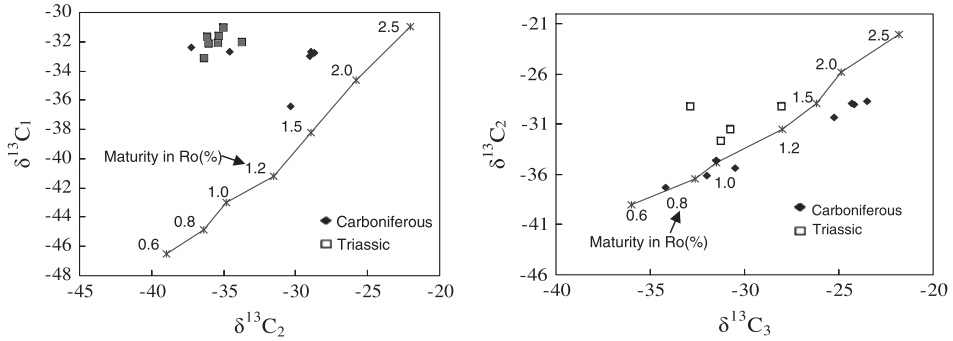

Fig. 5. Isotopic composition of methane against ethane and ethane against propane in natural gases of the Northeastern Sichuan Basin. The maturity line is according to a marine Kerogen ($\delta^{13}C = -33.65‰$) after Berner and Faber (1996). Diamond and square data points represent Carboniferous and Triassic gas samples, respectively. Numbers on the line of marine organic matter indicate the maturity of the source rock in%Ro.

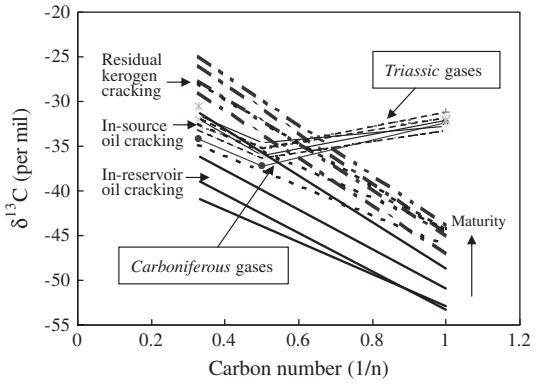

Fig. 6. An example of a natural gas plot using the method of Chung et al. (1988). The δ^{13}C values for the gas components δ^{13}Cn (n = 1–3) are plotted as a function of 1/n, where n is the number of carbon atoms in the molecule. The lines are extended to the intercept, which corresponds to the δ^{13}C values for the gas-producing groups in the kerogen. One sample obviously does not follow the linear trend: a mixture of source inputs, or heterogeneity in the source, would cause this deviation.

Carboniferous strata are estimated to be about 0.9–2.0%Ro and 0.8–2.2%Ro respectively, whereas the maturity of methane is estimated about 2.0–2.5%, i.e. much higher than those of ethane and propane.

To further delineate the gas mixtures in our case, we used the model of Chung et al. and plotted the results in Fig. 6. Chung et al. (1988) proposed a model to differentiate natural gases derived from a single source from those that are mixtures derived from two or more sources. The method is based on plotting the isotopic composition of methane through pentane as a function of the reciprocal carbon number of the hydrocarbon (Fig. 6). A linear fit to the data supports a co-genetic origin for the gas species, whereas a non-linear fit suggests that the gas accumulation is a mixture of gases, a chemically altered gas or a gas derived from a structurally heterogeneous carbon source. This model is commonly referred to as the natural gas plot.

In Fig. 6, three marine precursors of gases including in-reservoir oil, in-source oil and residual kerogen from our laboratory results were used and the isotopic compositions from methane to propane were plotted against the reciprocal carbon numbers together with results of Triassic and Carboniferous gases. Here, for clear differentiating the line trends, we choose a typical sample as the representative for each gas field. We found that mixing of gas sources occurred. The provenance of ethane and propane of both Carboniferous and Triassic gases is mainly from in-source oil cracking. They cannot derive from in-reservoir oil cracking because of their low maturity (Fig. 1). However, the maturities of methane are clearly higher than those of ethane and propane. As source for methane, we infer that the methane of Carboniferous gases may originate from high-matured residual kerogen whereas that of Triassic gases may come from both the high-matured residual kerogen and TSR-induced oil cracking.

To confirm the results of these geochemical diagrams, we examined micro-compositions of organic matter in some samples of source and reservoir rocks for both Carboniferous and Triassic gas systems. Abundant quantities of pyrobitumen were found in both source rocks and reservoir rocks, suggesting the secondary cracking of residual kerogen and oil. Fig. 7 shows some microscopic images, clearly confirming our results from gas molecular and isotopic identifications of gas origin. According to Xie, Tian, Wei, Li, and Yang (2005), pyrobitumens are widely found in the reservoir rock of the Triassic *Feixianguan* formation, the average content of pyrobitumen reaching 0.09–2.5%, which may be the residue left after oil cracking. Cai, Worden, Bottrell, Wang, and Yang (2003) and Liu et al. (2006) found natural sulfur-bearing immiscible inclusions firmly related to H_2S gas in oolite gas reservoir of *Feixianguan* formation, providing a solid support for TSR-induced oil cracking. For better understanding our geochemical results, we examined the burial history of a typical borehole (Well Shuishen-1) and the paleao-temperature evolution together with its maturity process simulated using PetroMod (version 11.0) in Fig. 8 (Lu et al., 2005). It is clear that the Triassic *Feixianguan* formation experienced high temperature of 150–200 °C in the geological history,

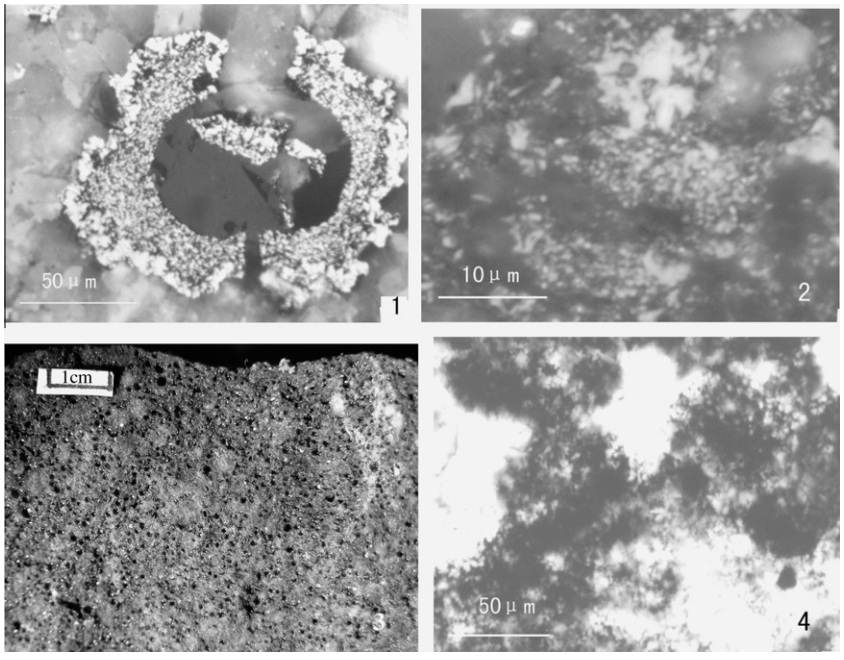

Fig. 7. Pyrobitumen in source rocks and reservoir rocks, NE Sichuan (1) pyrobitumen in reservoir rock, C_{2h},Well G-1, 4818 m, incident light, oil immersion; (2) pyrobitumen in source rocks, S_1, Well WK-1, 5258 m, incident light, oil immersion; (3) pyrobitumen in source rocks, P_2, Well PG-2, 4503 m, sample photo (4) pyrobitumen in reservoir rock, T_{1f}, Well Du-3, 4311 m, incident light, oil immersion.

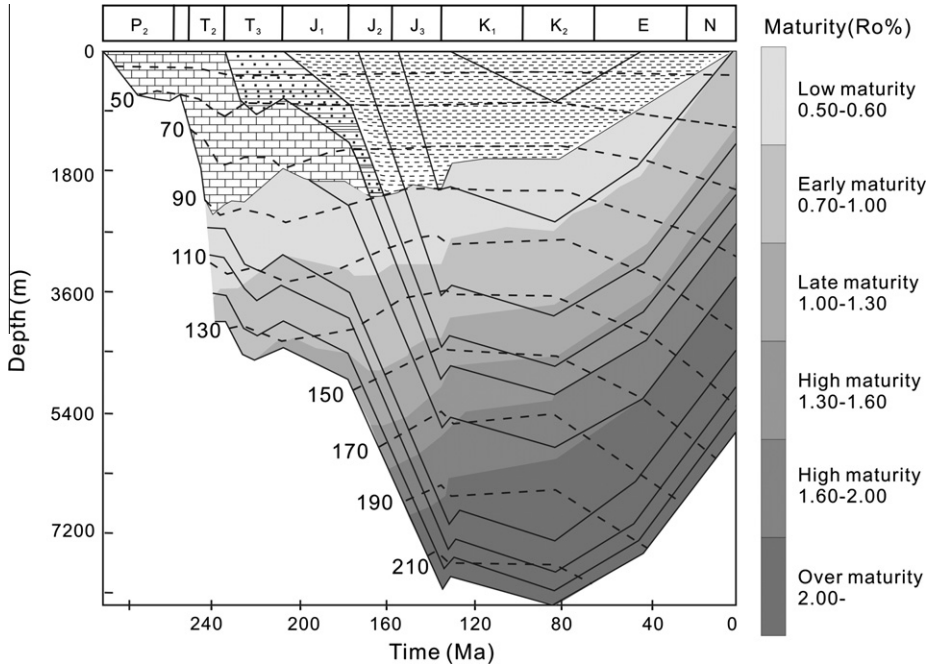

Fig. 8. The burial history of Well Shuishen-1 and the paleao-temperature and maturity (the solid line is the strata boundary and the dash line is the paleao-temperature in Centigrade, Modified from Lu et al., 2005).

which is sufficient for oil cracking and TSR reaction. Considering the geological characteristics of the studied area, the Silurian strata should be buried in more deep area have experienced much higher temperature history. The much higher maturity (over 3.0%Ro) of the borehole Silurian samples revealed by Ma et al. (2008) suggests that residual kerogen from Silurian marine shale and palaeo oils in Carboniferous reservoirs are the principal sources of Carboniferous gases in the Eastern Sichuan Basin, and the residual kerogen from Silurian and Permian marine rocks and the paleao oils in Permian and Triassic reservoirs are principal sources for Triassic gases in the Northeastern Sichuan Basin.

4. Conclusions

1. The $\delta^{13}C_1$ value of both Carboniferous and Triassic gases range between $-30‰$ to $-40‰$, suggesting weak isotopic fractionation in accordance with a biogenic origin including microbial or thermogenic ones. Relatively high $C_1/(C_2 + C_3)$ ratios related to strong compositional fraction suggest gas dryness to be mainly controlled by maturation and migration. The migration paths through porous weathered carbonate for Carboniferous oil and fault cracks for Triassic one may be the main factor controlling of migration fraction.
2. The $\ln(C_1/C_2)$ versus $\ln(C_2/C_3)$ diagram proposed by Prinzhofer and Huc (1995) can be used to identify primary cracking and secondary cracking gases as well as TSR-related gases. In NE Sichuan, Carboniferous gases and low-H_2S gases are mainly formed through secondary cracking of oil, whereas the high-H_2S gases are clearly related to the TSR (Thermal Sulfate Reduction) process, which promotes cracking of heavy hydrocarbons including ethane cracked into methane.
3. $\delta^{13}(C_1–C_2)$ diagram of Berner et al. in the study area clearly show an admixture of heavy (^{13}C-enriched) methane to the lower maturated ethane for the Triassic gas samples, while $\delta^{13}(C_2–C_3)$ diagram clearly suggest the same source and maturities ethane and propane for the Carboniferous gases and an admixture of heavy ethane to the propane for the Triassic gases.
4. The data plotting result in the diagram of Chung et al. (1988) shows a clear mixing of the gas sources. The ethane and propane of both Carboniferous and Triassic gases are mainly from the in-source oil cracking rather than the in-reservoir oil cracking. However, higher maturities of methane of Carboniferous gases may be from the high-matured residual kerogen and the methane of Triassic gases may be from both the high-matured residual kerogen and the TSR-induced oil cracking. Combining with the analysis of pyrobitumen and inclusions, it is deduced that the residual kerogen from Silurian marine shale and the palaeo oil reservoirs are main sources of the Carboniferous gases in Eastern Sichuan Basin, and the residual kerogen from Silurian and Permian marine rocks and the paleao oil reservoirs in Permian are main sources of the Triassic gases in Northeastern Sichuan Basin.

Acknowledgments

The authors thank the State Key Laboratory of Organic Geochemistry (SKLOG2012A02), China National S&T Major Project (2011ZX05008-002-13), GIGCAS 135 project (Y234021001), NSFC (40872091) and China 973 Program (2007CB209501) for the financial supports to this study. The authors greatly acknowledge Professor Tsanyao Frank Yang for his great help and two anonymous reviewers for their critical comments. Prof. Bernard de Jong of Utrecht University is greatly acknowledged for his help to improve the English of this manuscript. This is contribution No. IS-1564 from GIGCAS.

References

Bernard, B.B., Brooks, J.M., Sackett, W.M., 1978. Light hydrocarbons in recent Texas continental shelf and slope sediments. Journal of Geophysics Research 83, 4053–4061.

Berner, U., Faber, E., 1996. Empirical carbon isotope/maturity relationships for gases from algal kerogens and terrigenous organic matter, based on dry, open-system pyrolysis. Organic Geochemistry 24, 947–955.

Cai, C.F., Worden, R.H., Bottrell, S.H., Wang, L.S., Yang, C.C., 2003. Thermochemical sulphate reduction and the generation of hydrogen sulphide and thiols (mercaptans) in Triassic carbonate reservoirs from the Sichuan Basin, China. Chemical Geology 202, 39–57.

Chung, H.M., Gormly, J.R., Squires, R.M., 1988. Origin of gaseous hydrocarbons in subsurface environments: theoretical considerations of carbon isotope distribution. Chemical Geology 71, 97–104.

Dai, J.X., Zou, C.N., Qin, S.F., Tao, S.Z., Ding, W.W., Liu, Q.Y., et al., 2008. Geology of giant gas fields in China. Marine and Petroleum Geology 25, 320–334.

Hu, G.C., 1997. A breakthrough of oil–gas exploration of sichuan basin – a case study. Marine Origin Petroleum Geology 3, 52–53 (in Chinese).

Liu, D.H., Xiao, X.M., Xiong, Y.Q., Geng, A.S., Shen, J.G., Wang, Y.P., et al., 2006. Origin of natural sulphur-bearing immiscible inclusions and H_2S in oolite gas reservoir in Feixianguan, Sichuan. Science in China series D Earth Science 49, 242–257.

Lu, Q.Z., Hu, S.B., Guo, T.L., Li, Z.P., 2005. The background of the geothermal field for formation of abnormal high pressure in the Northeastern Sichuan Basin. Chinese Journal of Geophysics 5, 1110–1116 (in Chinese).

Ma, Y.S., Zhang, S.C., Guo, T.L., Zhu, G.Y., Cai, X.Y., Li, M.W., 2008. Petroleum geology of the Puguang sour gas field in the Sichuan Basin, SW China. Marine and Petroleum Geology 4–5, 357–370.

Prinzhofer, A., Huc, Y., 1995. Genetic and post-genetic molecular and isotopic fractionations in natural gases. Chemical Geology 126, 281–290.

Wang, L.S., Li, Z.Y., Shen, P., Chen, S.J., Zhang, J., Xie, B.H., 2004. On the hydrocarbon generation conditions of the large and middle scale gas fields in Eastern part of Sichuan Basin. Natural Gas Geoscience 6, 567–571 (in Chinese).

Wang, Y.G., Chen S.J., Xu, SQ, 2001. Conditions of reservoir formation and exploration technology of natural gas in the Paleozoic-Upper Proterozoic series of the Sichuan Basin. Petroleum Industry, Beijing, pp. 1.

Wang, Y.P., Wang, Z.Y., Zhao, C.Y., Wang, H.J., Liu, J.Z., Lu, J.L., et al., 2007. Kinetics of hydrocarbon gas generation from marine kerogen and oil: implications for the origin of natural gases in the Hetianhe Gasfield, Tarim Basin, NW China. Journal of Petroleum Geology 4, 339–356.

Wang, Y.P., Zhao, C.Y., Wang, Z.Y., Wang, H.J., Tian, J., Zou, Y.R., et al., 2008. Identification of marine natural gases with different origin sources. Science in China Series D – Earth Sciences 1 (Suppl.), 148–164.

Wang, Y.P., Zhang, S.C., Wang, F.Y., Wang, Z.Y., Zhao, C.Y., Wang, H.J., et al., 2006. Thermal cracking history by laboratory kinetic simulation of Paleozoic oil in eastern Tarim Basin, NW China, implications for the occurrence of residual oil reservoirs. Organic Geochemistry 37, 1803–1815.

Wang, Y.P., Dai, J.X., Zhao, C.Y., Liu, J.Z., 2010. Genetic origin of Mesozoic natural gases in the Ordos Basin (China): comparison of carbon and hydrogen isotopes and pyrolytic results. Organic Geochemistry 4, 1045–1048.

Xie, Z., Ding, Y., Luo, Q., 2000. Development prospection of natural gases of Sichuan Basin at 21th century. Natural Gas Industry 6, 1–6 (in Chinese).

Xie, Z., Tian, S., Wei, G., Li, J., Yang, W., 2005. The study on bitumen and foregone pool of Feixianguan oolitic in Northeast Sichuan Basin. Natural Gas Geoscience 3, 283–288 (in Chinese).

Zhang, S.C., Zhu, G.Y., 2006. Gas accumulation characteristics and exploration potential of marine sediments in Sichuan Basin. Acta Petrolei Sinica 5, 1–8 (in Chinese).

Zhao, W.Z., Wang, Z.C., Wang, Y.G., 2006. Formation mechanism of highly effective gas pools in the Feixianguan Formation in the NE Sichuan Basin. Geological Review 5, 708–718.